FEA Mechanical Modeling of Torque Transfer Components for Fully Superconducting Rotating Machines

Tingcheng.Wu[1], Guillaume.Escamez[1], Clement.Lorin[1], Philippe J. Masson[1]
[1]University of Houston
*Mechanical Engineering, N272 Engineering Bldg 1, Houston, TX-77004, wutingcheng29@gmail.com

Abstract: Because of their very high specific torque, fully superconducting rotating machines are considered as enabling technology for future turbo-electric propulsion for transportation aircraft. NASA is funding the development of a high fidelity fully superconducting machine sizing tool able to generate optimized designs based on power requirements and design constraints. The model developed includes a realistic 3D geometry representation and is based on parametric design methods. COMSOL MultiPhysics has been used to validate the mechanical calculations including the thermal stress, strain, displacement and torque induced stress and deformation. This parametric model allows us to get the relationship between stress/strain and a series of parameters. This will help define the most proper materials considering different required working conditions. The simulations allowed for a full characterization of the superconducting motor composite shaft and successfully validated the analytical estimation of the stress and deformation of the shaft during cool down and under the effect of the applied torque.

Keywords: Torque Transfer, Heat Transfer, Thermal Stress, Deformation.

1. Introduction

Fully superconducting rotating machines for future turbo-electric propulsion require high torque and power to weight ratio. The weight and size of the machine need to be minimized during design. Superconductors can only operate at cryogenic temperatures in the 20-40K range. The torque transfer components need to transmit mechanical torque between cryogenic and room temperature and, as a result, is exposed to high temperature gradient. Therefore, special care needs to be taken towards simulation of the temperature distribution, conducted heat and thermal stress distribution in the shaft.

The work presented deals with a realistic 3D geometry representation of the rotor shaft of a superconducting motor. A fully parameterized model was implemented in COMSOL MultiPhysics, which allows for parametric sweeps during the optimization process.

This paper mainly discusses the temperature distribution, stress distribution, thermal stress and torque induced stress in steady-state nominal operation of the machine. With the help of COMSOL MultiPhysics, we can identify the parameters that have significant influence on stress distribution.

1.1 Model geometry and Material

Figure 1 shows the general geometry of the shaft. The shaft consists of 5 separated parts connected by bolts. Poles are protruding to accommodate the superconducting winding (not represented in figure 1).

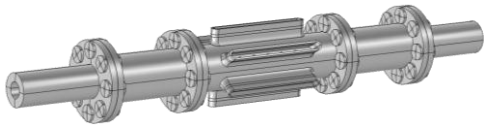

Figure 1. Torque transfer components model

Because the rotor houses superconducting coils, the temperature needs to be maintained lower than 20 K to keep the winding in the superconducting state with an acceptable critical current density. The two ends of the shaft are at room temperature (300K) and connected to the mechanical load. Thus, there will be a large temperature gradient between the winding parts and the two shaft end sections. In order to thermally insulate the section at cryogenic temperature, different materials are used for different parts of the shaft. As shown in Figure 2 , the two blue parts are composed of G10 material with low thermal conductivity to take most of the temperature gradient. G10 is a widely used glass fiber material in cryogenic applications because

of its low thermal conductivity and relatively high yield stress. All other parts in gray in figure 2 are made of Stainless Steel 316. Non-magnetic metal sections are required to accommodate vacuum seals and bearings.

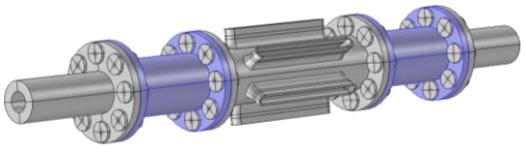

Figure 2. Materials composing the shaft

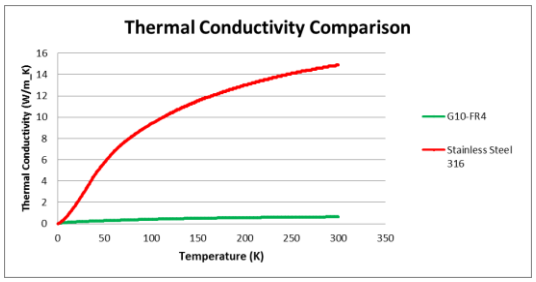

Figure 3. Thermal Conductivity Comparison

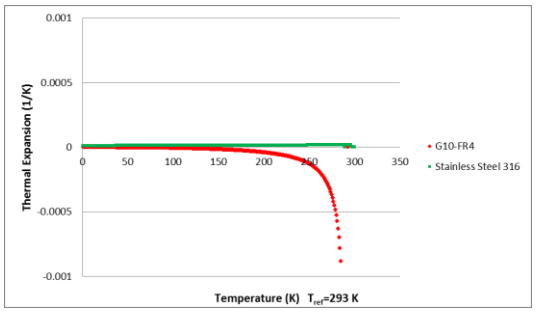

Figure 4. Thermal Expansion Coefficient

Figure 3 shows the thermal conductivities of G10 and stainless steel 316, which means compared with Stainless Steel 316; the G10 part will take most of the temperature gradient and thermally insulate the active part of the rotor. The low operating temperature will also cause shrinkage of the whole shaft; each part have a different coefficient of thermal expansion leading to thermally induced stress. Figure 4 shows the thermal expansion coefficients of the two materials used (T_{ref} = 293K). When temperature is lower than 200K, the two materials have almost the same thermal expansion coefficients, however, when the temperature is over 200K, the difference of thermal expansion coefficients is significant. Figure 5 shows the elongation ratio of the two materials used when the temperature changes (T_{ref} = 0K).

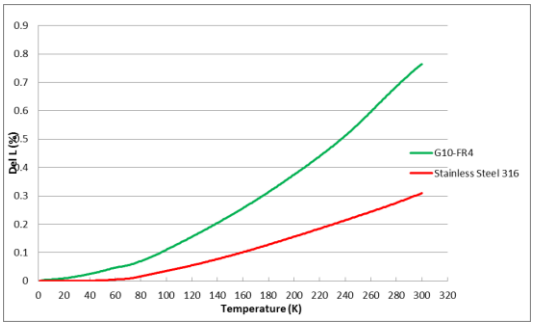

Figure 5. Materials' ΔL with Temperature Change

2. Numerical solution

The case is a coupled problem of heat transfer and solid mechanics. Thus, we used two modules in COMSOL MultiPhysics, Heat Transfer in Solids and Solid Mechanics.

We created a study with two steps:

- Step1 uses the *Heat Transfer in Solids* module, calculates the temperature distribution in the whole shaft.

- Step2 uses the *Solid Mechanics* module, particularly thermal expansion and linear elasticity. We coupled the *Heat Transfer in Solid* module with the *Solid Mechanics* module to get the thermal stress.

We present the stationary analysis of the system, including nominal steady state temperature distribution, steady state stress distribution as well as the displacement.

2.1 Governing equation

The unsteady heat conduction with thermo-elasticity is described by the following governing equation:

$$\rho C_p u \cdot \nabla T_2 = \nabla \cdot (k \nabla T_2) + Q \qquad (1)$$

Where T_2 is the temperature, C_p is the heat capacity under constant pressure; k is the thermal conductivity, ρ is the material density, Q is the heat source.

Boundary conditions at both ends of the shaft are:

$T = T_0$

Where T_0 is the initial value of temperature et as 300K, and the initial value for cryogenically cooled parts is set as 20K.

In the Solid Mechanics module, we take two factors into consideration: Thermal Stress and Torque induced Stress.

For the Thermal Stress, we use the following governing equation:

$s - S_0 = C: (\varepsilon - \varepsilon_0 - \varepsilon_{inel}), \varepsilon_{inel} = \alpha (T - T_{ref})$

3. Simulation results

3.1 Heat Transfer in Solids

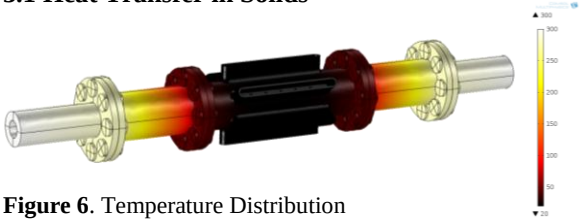

Figure 6. Temperature Distribution

Figure 6 show the steady state temperature distribution in the whole shaft after cool-down. As predicted, most of the temperature gradient is in the G10 components. The two ends of the shaft are at room temperature (300K), while the central section composed of stainless steel is around 20K., which can ensure the superconducting properties of the superconductive material.

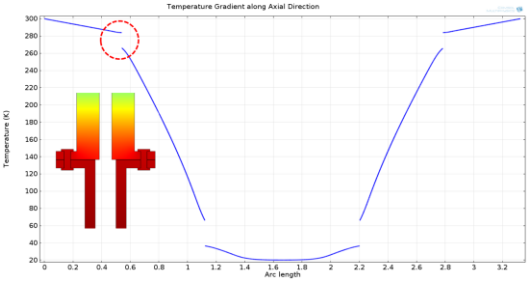

Figure 7. Temperature Gradient along Axial Direction

Figure 7 shows the temperature gradient along the axial direction of the shaft. Discontinuities occur because of the poor thermal contact between the different parts. The poor thermal contact is achieve through a rough surface finish of the adjacent parts and is modelled through the definition of pairs in COMSOL. The poor contacts act as further thermal insulation. Figure 7 also shows that temperature gradient in each part is almost linear.

3.2 Solids Mechanics

Stress distribution is the key point of interest. The peak value of the stress and its location is very important to the whole shaft design. Figure 8 shows the local value of the displacement as well as the dimension change of the shaft. The 3 meter long shaft is about 8 mm shorter after cool-down.

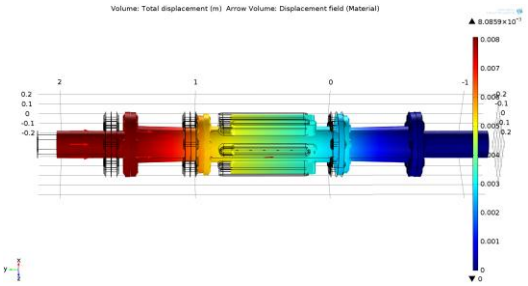

Figure 8. Deformation of the Shaft

The stress comes from two different phenomena: thermal stress due to mismatched CTEs and mechanically induced stress due to the electromagnetic torque in the motor. We conducted series of simulations to find the relationship between those two stresses and the maximum stress value in the shaft. Several simulations were run with the thermal and mechanical analyses decoupled. Table 1 shows the thermal stress and torque induced stress. It is apparent that the peak value of thermal stress is almost 100 times greater than the torque induced stress for this specific design. Thus, the first step of the design process should be focused on the thermal stress.

Torque(Nm)	Max Stress(N/m^2)	Thermal Stress ONLY(N/m^2)	Torque induced stress ONLY(N/m^2)
3000	4.44E+10	4.44E+10	3.0200E+07
4000	4.44E+10	4.44E+10	6.6900E+07
5000	4.45E+10	4.44E+10	1.0350E+08
6000	4.45E+10	4.44E+10	1.4030E+08
7000	4.45E+10	4.44E+10	1.7700E+08
8000	4.46E+10	4.44E+10	2.1390E+08
9000	4.46E+10	4.44E+10	2.5070E+08
10000	4.46E+10	4.44E+10	2.8770E+08
11000	4.47E+10	4.44E+10	3.2460E+08
12000	4.47E+10	4.44E+10	3.6160E+08

Table 1. Thermal stress and Torque induced Stress

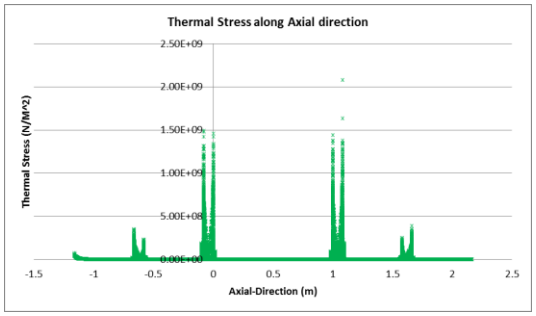

Figure 9. Thermal stress distribution along axial direction

Figure 9 shows the thermal stress distribution in the shaft along the axial direction when we run the pure thermal stress simulations. In this case, we just couple the heat transfer with thermal expansion in linear elastic property. One end of the shaft is fixed and the other one free, then the stress calculated is only caused by the heat transfer (temperature gradient) in the shaft.

There are several factors that will affect the thermal stress in the bolts: material, number of bolts, connection conditions and cross section area of the bolts.

- Material: the application requires the use of non-magnetic materials such as stainless steel, titanium, etc. In this case, we decided to use stainless steel 316.

- Number of bolts: previous research[1] shows that with the increase of the number of bolts, the maximum thermal stress will also increase. Thus, we reduced the number of connection bolts from 8 to 3.

- Connection conditions: to represent thermal insulation of the bolts, we defined low thermal conductivity sheets between the connected faces. The function of those sheets can also be seen in Figure 7.

Cross section area of the bolts: in order to get the relationship between the cross section area and the thermal stress, we ran a series of simulations. We defined a parameter *d* representing the gap between the bolts and the holes. While keeping the size of the hole, we changed the value of parameter *d* to get a different cross section for the bolts.

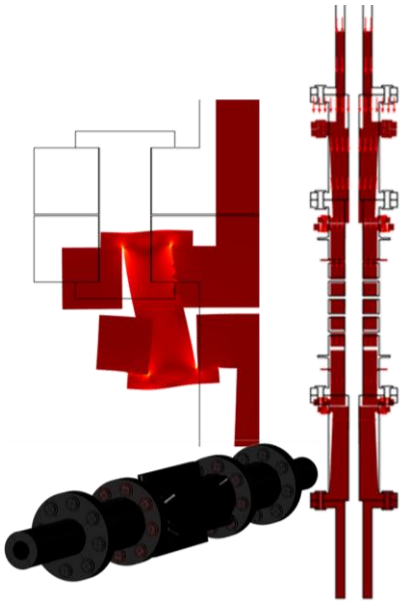

Figure 10. Stress and Deformation

Figure 10 shows that the maximum stress occurs in the bolts connecting the G10 and stainless steel parts. As a result, we focused on the design of the connection bolts.
Figure 10 shows that with the decrease of the bolt cross section area, the average thermal stress also decreased. The peak stress value extracted from the simulation shows large variations which we associated with artificial stress concentration in low mesh density areas. As a result, we decided to describe the stress change more accurately by considering the average stress change in the bolts as a reference.

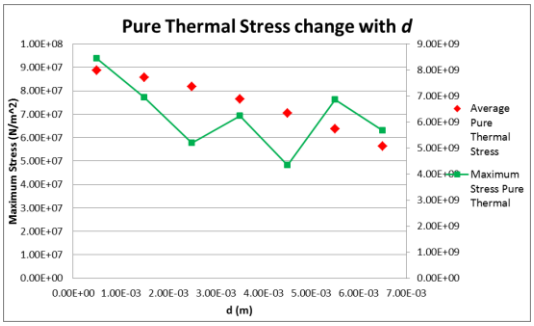

Figure10. Pure thermal stress change with parameter *d*

We conduct a parametric sweep simulation including both the thermal and torque induced

stresses for different values of *d*; the results are shown in Figure 11.

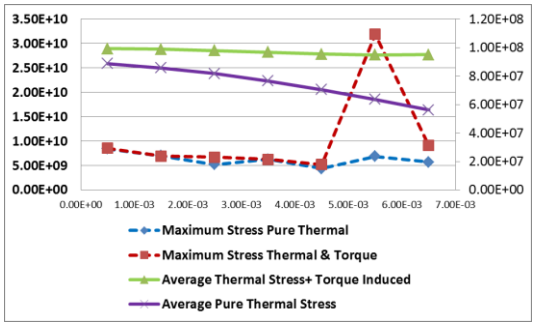

Figure 11. Parametric Sweep Results

From Figure 11, we can find the general trend of the stress with the change of cross section area of the bolts. The only singular point in maximum stress with the effect of temperature and torque is likely coming from numerical error and poor localized mesh density. As to the average stress in the bolts, it is found that the stress in the bolts decreases with the decrease of cross section area.

4. Conclusion

By using the COMSOL Multiphysics, we obtained the temperature and stress distribution in the shaft of a superconducting machine. Additionally, with the help of the parametric sweep function, we obtained the trends of the stress in the shaft components affected by different operating factors. The results show that the cross section area of the bolt connecting parts made of different materials has a significant influence on the peak thermal stress.

5. References

1. Yifan Chen, Research on Thermal Contact Resistance of Bolt-Jointed Interface and Heat Conduction Characteristics of Aluminum Honeycombs (2002)

2. R.A. Jones, Mechanical shimming of resistive or superconductive magnets for magnetic resonance imaging, Magnetic Resonance Imaging, **Volume 3** (1985)

3. Marco Cavenago and Giovanni Bisoffi, Optimization studies of a 14.4 GHz ECR ion source for the superconductive linac at Legnaro, Nuclear Instruments and Methods in Physics Research (1991)

4. B. J. Maddock, G. B. James, and W. T. Norris, Superconductive composites Heat transfer and steady state stabilization, CRYOGENICS (1969)